Available online at www.sciencedirect.com
ScienceDirect
Trans. Nonferrous Met. Soc. China 25(2015) 2630−2636
Transactions of Nonferrous Metals Society of China
www.tnmsc.cn

Thermodynamics and characterization of shape memory Cu−Al−Zn alloys

Lidija GOMIDŽELOVIĆ[1], Emina POŽEGA[1], Ana KOSTOV[1], Nikola VUKOVIĆ[2], Vesna KRSTIĆ[1], Dragana ŽIVKOVIĆ[3], Ljubiša BALANOVIĆ[3]

1. Mining and Metallurgy Institute, Zeleni Bulevar 35, Bor 19210, Serbia;
2. Faculty of Mining and Geology, University of Belgrade, Đušina 7, Belgrade 11000, Serbia;
3. Technical Faculty in Bor, University of Belgrade, VJ 12, Bor 19210, Serbia

Received 14 August 2014; accepted 8 November 2014

Abstract: The thermodynamic properties and the microstructure, hardness and electrical conductivity of shape memory alloys (SMAs) belonging to ternary Cu−Al−Zn system were studied by Muggianu model and experiment, respectively. The isothermal section of phase diagram at 293 K was calculated using Thermo-Calc software. Experiments were conducted by X-ray diffraction, light optic microscopy, scanning electron microscopy with energy dispersive X-ray spectrometry, hardness and electrical conductivity measurements. The calculated values of thermodynamic properties indicate that Cu shows good miscibility with Al and Zn in all investigated alloys. The microstructural analysis of samples reveals that the structure consists of large and polygonal grains.
Key words: thermodynamics; shape memory alloy; Cu−Al−Zn alloys; hardness; electrical conductivity

1 Introduction

Alloys belonging to ternary Cu−Al−Zn system are mostly used like Cu-based shape memory materials [1−4], but as well have application in catalysis [5, 6], electronics [7] and production of metal matrix composites [8]. Also, different multicomponent alloys are based on this ternary system [9, 10]. The properties linked to shape memory behavior of Cu−Al−Zn alloys, like martensitic transformation [11−15] and shape memory effect [16−18], have been thoroughly researched. Additionally, the properties like corrosion behavior [19], microstructure and mechanical properties of selected Cu−Al−Zn alloys have been investigated [20−23]. The phase diagram of Cu−Al−Zn system, due to technical importance, has been investigated by lots of researchers, and most recent review of this data was conducted by LIANG and CHANG [24].

Thermodynamic properties of ternary Cu−Al−Zn system have been experimentally investigated by SEBKOVA and KUBICEK [25] using electromotive force method, by SUGINO and HAGIWARA [26] using isopiestic method and by VAN et al [27] using electromotive force method. The thermodynamic description of Cu−Al−Zn in the Cu-rich corner was given by MIETTINEN [28]. Also, a general solution model [29] and Redlich−Kister−Muggianu model [30] were used for the calculation of thermodynamic properties of Cu–Al–Zn ternary system. Within the computational phase studies of quaternary Al−Cu−Mg−Zn system, SEIFERT et al [31] calculated isothermal section at 673 K. Recently, ALDIRMAZ et al [32] performed SEM and X-ray diffraction studies on the microstructures of Cu−26.04%Zn−4.01%Al alloy.

The objective of this work is to supplement the knowledge of thermodynamic properties, microstructure, mechanical and electrical properties of shape memory alloys belonging to Cu−Al−Zn ternary system, taking into account the fact that these properties are not well represented in other literature.

2 Theoretical

There are many methods for calculating thermodynamic properties of ternary systems based on information about binary systems included in their composition. For calculating thermodynamic properties

Foundation item: Projects (34005, 172037) supported by the Ministry of Education, Science and Technological Development of the Republic of Serbia
Corresponding author: Lidija GOMIDŽELOVIĆ; Tel: +381-30-454268; Fax: +381-30-435175; E-mail: lgomidzelovic@yahoo.com
DOI: 10.1016/S1003-6326(15)63885-7

of Cu−Al−Zn system in this work, two different models were considered: Toop [33] as asymmetric model and Muggianu [34] as symmetric model. The basic theoretical interpretations of mentioned models are given as follows:

Toop model:

$$\Delta G^{\mathrm{E}}=\frac{x_2}{1-x_1}\Delta G_{12}^{\mathrm{E}}(x_1;1-x_1)+\frac{x_3}{1-x_1}\Delta G_{13}^{\mathrm{E}}(x_1;1-x_1)+(x_2+x_3)\Delta G_{23}^{\mathrm{E}}\left(\frac{x_2}{x_2+x_3};\frac{x_3}{x_2+x_3}\right) \quad (1)$$

Muggianu model:

$$\Delta G^{\mathrm{E}}=\frac{4x_1x_2}{(1+x_1-x_2)(1+x_2-x_1)}\cdot\Delta G_{12}^{\mathrm{E}}\left(\frac{1+x_1-x_2}{2};\frac{1+x_2-x_1}{2}\right)+\frac{4x_2x_3}{(1+x_2-x_3)(1+x_3-x_2)}\cdot\Delta G_{23}^{\mathrm{E}}\left(\frac{1+x_2-x_3}{2};\frac{1+x_3-x_2}{2}\right)+\frac{4x_3x_1}{(1+x_3-x_1)(1+x_1-x_3)}\Delta G_{31}^{\mathrm{E}}\left(\frac{1+x_3-x_1}{2};\frac{1+x_1-x_3}{2}\right) \quad (2)$$

In all given equations, ΔG^{E} and $\Delta G^{\mathrm{E}}_{ij}$ correspond to the integral molar excess Gibbs energies for ternary and binary systems, respectively, while x_1, x_2, x_3 correspond to the mole fraction of components in the investigated ternary system.

3 Experimental

The samples were obtained from industrial production. The compositions, shapes and production methods of investigated samples are given in Table 1.

The microstructural analysis of investigated samples was performed by light optical microscopy (LOM) using a Reichert MeF2 microscope, and by SEM−EDX using a JEOL JSM−6610LV scanning electron microscope coupled with an Oxford instrument X−Max 20 mm^2 SDD energy-dispersive X-ray spectrometer. Prior to metallographic analysis, the surfaces of the polished samples were etched with $FeCl_3$+HCl+H_2O solution to reveal the structure of investigated alloys. Series of overall (macro) hardness measurements were done using standard procedure according to Vickers, with a load of 100 N. The electrical conductivity of investigated materials was measured using the standard apparatus–SIGMATEST 2.069 (Foerster) eddy current instrument (the measuring probe diameter is 8 mm). The X-ray diffraction patterns of powder samples were taken by an X-ray diffraction (XRD) model explorer, GNR with X-ray tube Cu K_α (λ=1.541874 Å). The operating conditions were voltage of 40 kV and current of 30 mA with step size of 0.05. The configuration is θ–θ geometry.

4 Results and discussion

For the purpose of further calculation, the basic thermodynamic information by constitutive subsystems in the Cu−Al−Zn system was taken from Refs. [35−37], and presented in the form of Redlich−Kister parameters listed in Table 2.

The first step in calculation was to determine which of two considered models are more appropriate for the calculation of thermodynamic properties of ternary Cu−Al−Zn system. This was achieved by comparing the available literature data (Fig. 1). Analyzing dependence of Al activity from composition presented in Fig. 1, it can be observed that the values of Al activity obtained using Muggianu model show reasonably good agreement

Table 1 Compositions, shapes and production methods of investigated samples

Sample	Mole fraction/%			Shape	Production method
	Cu	Al	Zn		
A1	73.0	4.0	23.0	Wire (d16 mm)	Cast in graphite molds
A2	71.0	4.6	24.4	Wire (d20 mm)	Up-cast
A3	75.1	8.3	16.6	Wire (d20 mm)	Up-cast

Table 2 Redlich−Kister parameters for constitutive binary systems

System ij	L_{ij}^0	L_{ij}^1	L_{ij}^2	L_{ij}^3	Ref.
Al−Cu	−67094+8.555T	32148−7.118T	5915−5.889T	−8175+6.049T	[35]
Cu−Zn	−40695.54+12.65269T	4402.72−6.55425T	7818.1−3.25416T	0	[36]
Al−Zn	10465.55−3.39259T	0	0	0	[37]

T stands for temperature.

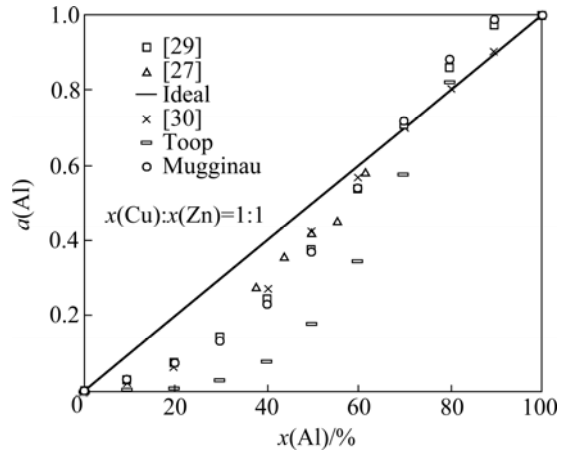

Fig. 1 Dependence of Al activities from composition at 1123 K, calculated using Toop and Muggianu models compared with Refs. [27, 29, 30]

with Refs. [27, 29, 30], which is not the case with the values obtained using Toop model. According to this, it can be concluded that ternary Cu−Al−Zn system belongs to a group of geometrical "symmetric" systems, so Muggianu model should be used to calculate its thermodynamic properties.

Taking the composition of investigated samples into account, two cross sections from Cu corner were selected for the calculation of thermodynamic properties, section x(Al):x(Zn)=1:5 and x(Al):x(Zn)=1:2. The calculation was conducted at 1400 K, because at this temperature all metals are in liquid state (Cu is metal with the highest melting point in investigated ternary Cu−Al−Zn system equals to 1357 K [38]).

The partial thermodynamic quantities of Cu, Al, and Zn are calculated according to the equations:

$$G_i^{\mathrm{E}} = G^{\mathrm{E}} + (1 - x_i)(\partial G^{\mathrm{E}} / \partial x_i) = RT \ln \gamma_i \quad (3)$$

and

$$a_i = x_i \gamma_i \quad (4)$$

where a_i is the activity of component i, x_i is the mole fraction of component i, γ_i is the activity coefficient of component i.

The calculated integral molar Gibbs excess energies (ΔG^{E}) and activities of the investigated system Cu−Al−Zn along selected sections and at given temperature are presented in Fig. 2. All thermodynamic properties calculated are related to the liquid phase.

The values for excess integral Gibbs energy of investigated sections are negative, with the minimum value up to −9 kJ/mol for section x(Al):x(Zn)=1:2. The values of Cu activity show negative deviation from the Rault's law at 1400 K for both investigated section. Based on the values of thermodynamic properties

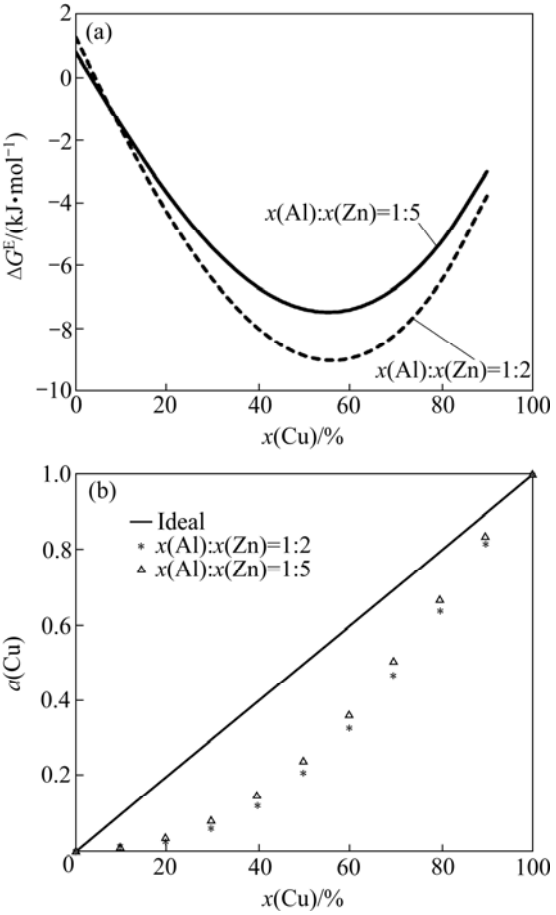

Fig. 2 Results of thermodynamic calculation using Muggianu model for cross-sections x(Al):x(Zn)=1:5 and x(Al):x(Zn)=1:2 at 1400 K: (a) Integral molar Gibbs excess energies; (b) Cu activity

obtained by calculations, it can the concluded that Cu as the main alloying element in the investigated alloys shows good miscibility with Al and Zn. Additionally, the isothermal section of ternary Cu−Al−Zn phase diagram at 298 K (Fig. 3) is calculated using Thermo-Calc software [39,40] developed by Thermo-Calc software AB based on Calphad [41,42] approach. All calculations are based on thermodynamic data which are supplied in a database SSOL5. Assessed and calculated isothermal sections of ternary Cu−Al−Zn system at 700 °C and 500 °C from Ref. [24] have been compared with corresponding isothermal sections calculated using the database SSOL5 and sufficient similarity was detected, leading to the conclusion that SSOL5 database contains data appropriate for this calculation.

Thirteen different phases can be identified in isothermal section of ternary Cu−Al−Zn system (Fig. 3) and most of them can be connected to phases found in constitutive binary systems: Cu−Al, Cu−Zn and Al−Zn [43], but there are also ternary phases which are characteristic for this ternary system.

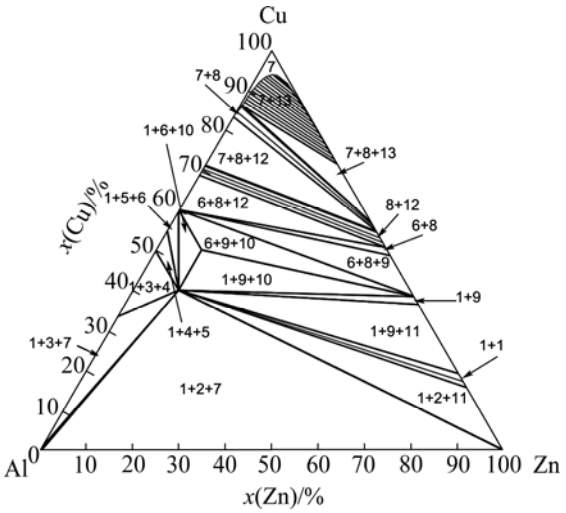

Fig. 3 Calculated isothermal section of ternary Cu−Al−Zn phase diagram at 298 K (obtained using Thermo-Calc 3.0): 1—AlCuZn_Tau; 2—HCP_Zn; 3—AlCu_Theta; 4—AlCu_Eta; 5—AlCu_Zeta; 6—AlCu_Delta; 7—FCC_L12; 8—BCC_B2; 9 — CuZn_Gamma; 10 — AlCuZn_Tau#2; 11 — HCP_A3; 12—D_Gamma; 13—FCC_L12#2

The XRD pattern of Sample A1 is shown in Fig. 4. The diffraction pattern represents the crystal lattice of the α-solid solution CuZnAl phase with FCC (surface-centered cubic lattice) with the presence of β phase in traces. According to the chemical composition of investigated alloy, it can be expected that alloy consists of two phases (α and β), which is confirmed by the obtained XRD pattern.

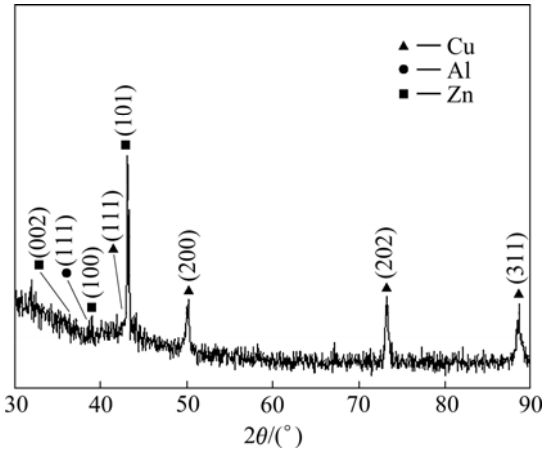

Fig. 4 XRD pattern of Sample A1

The results of microstructural analysis using light optical microscopy and SEM−EDX for Sample A1 are given in Fig. 5. The chemical compositions determined by EDX analysis are presented in Table 3. The optical microscopy reveals that the microstructure of Sample A1 consists of polygonal and irregularly shaped grains.

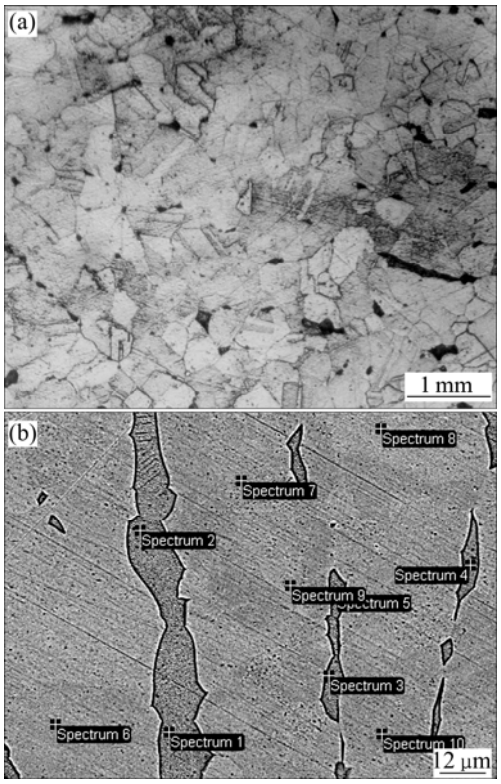

Fig. 5 Microstructures of sample A1: (a) LOM image; (b) SEM−EDX image

Table 3 Results of SEM−EDX analysis of Sample A1

Spectrum	Mole fraction/%		
	Al	Cu	Zn
1	5.66	69.67	24.67
2	5.23	70.85	23.93
3	5.67	71.21	23.12
4	4.29	73.97	21.74
5	4.36	73.33	22.31
6	3.90	73.69	22.41
7	3.79	73.78	22.42
8	3.65	74.52	21.82
9	3.55	74.09	22.36
10	3.98	73.72	22.30

The results of microstructural analysis using light optical microscopy and SEM−EDX for Sample A2 are given in Fig. 6. The chemical compositions determined by EDX analysis are presented in Table 4. Large and elongated grains characterize the microstructures of Sample A2 (Fig. 6(a)).

The results of microstructural analysis using light optical microscopy and SEM−EDX for Sample A3 are given in Fig. 7. The chemical compositions determined by EDX analysis are presented in Table 5. The microstructure of Sample A3, examined by optical

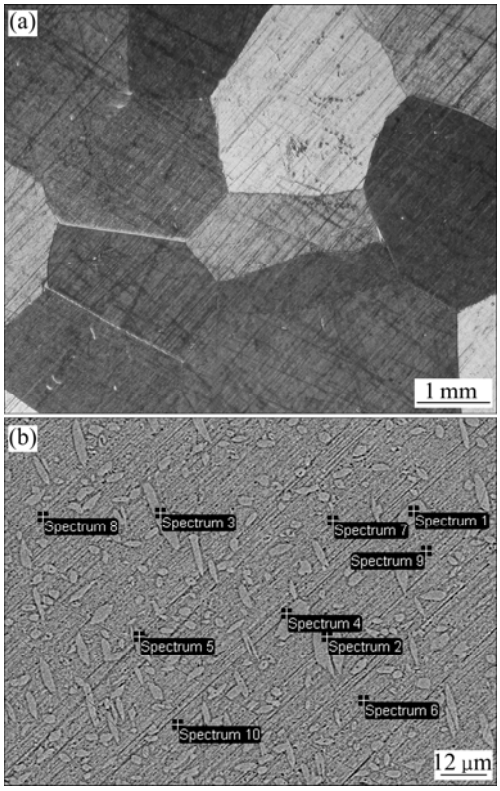

Fig. 6 Microstructures of Sample A2: (a) LOM image; (b) SEM−EDX image

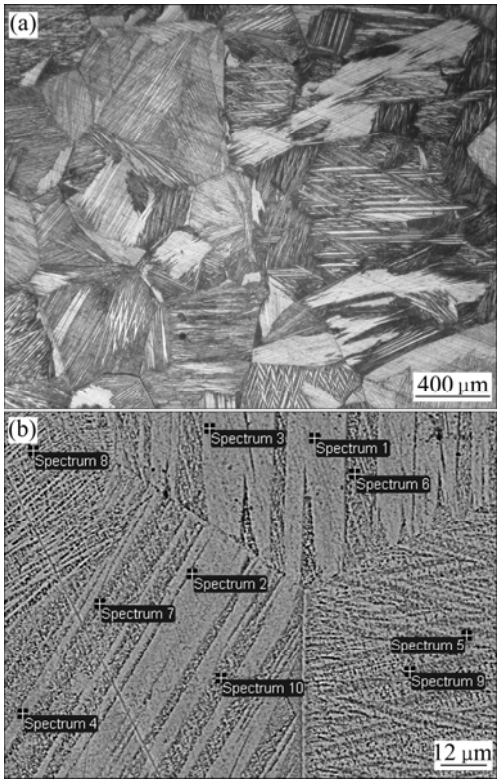

Fig. 7 Microstructures of Sample A3: (a) LOM image; (b) SEM−EDX image

Table 4 Results of SEM−EDX analysis of Sample A2

Spectrum	Mole fraction/%		
	Al	Cu	Zn
1	4.14	73.02	22.85
2	4.10	73.69	22.21
3	4.18	72.63	23.19
4	4.11	72.49	23.40
5	3.72	72.85	23.42
6	5.13	69.01	25.86
7	5.04	69.29	25.68
8	5.41	68.75	25.84
9	5.83	68.52	25.65
10	4.68	69.54	25.78

Table 5 Results of SEM−EDX analysis of Sample A3

Spectrum	Mole fraction/%		
	Al	Cu	Zn
1	8.33	76.59	15.08
2	8.08	74.73	17.19
3	8.40	75.54	16.06
4	7.99	74.98	17.03
5	9.55	73.41	17.04
6	8.17	75.25	16.58
7	8.33	74.93	16.74
8	8.25	74.99	16.76
9	6.30	76.83	16.87
10	9.44	73.91	16.65

microscopy (Fig. 7(a)), reveals large and polygonal grain structure. The closer look provided by SEM images (Fig. 7(b)) reveals different crystallization patterns inside every grain.

According to the phase diagram of binary Cu−Zn and Cu−Al systems [43], the solid solubility of Al in Cu is approximately 18% (mole fraction), and for Zn which goes up to 30% (mole fraction). Considering that, for all investigated samples, the base material is Cu (65%−75% Cu, mass fraction). It is reasonable to expect that Al and Zn will dissolve in Cu, creating solid solutions. That is confirmed by the results of EDX analysis presented in Tables 3−5 and the XRD pattern of Sample A1 (Fig. 4). The EDX results as well indicate that the homogeneity of samples is satisfactory, as the chemical compositions of different measuring points do not vary too much.

The results of Vickers hardness measurements of investigated Cu−Al−Zn alloy samples are given in Table 6. Three sets of measurements were conducted and the average value was calculated. The decrease of hardness values with increasing the Al content in alloy can be noticed.

The results of electrical conductivity measurements are presented in Table 7. Five sets of measurement were conducted and the mean value of electrical conductivity was calculated based on the obtained values.

Table 6 Hardness of investigated Cu−Al−Zn alloys

Sample	HV_{10}			
	1	2	3	Mean value
A1	264	254	251	256.3
A2	201	222	240	212
A3	153	159	151	154.3

Table 7 Measured values of electrical conductivity of investigated Cu−Al−Zn alloys

Sample	Electrical conductivity/(10^6 S·m^{-1})					
	1	2	3	4	5	Mean value
A1	11.1	11.3	11.2	11.4	11.3	11.26
A2	10.4	11.0	9.4	10.8	9.0	10.12
A3	10.6	10.3	10.5	10.35	10.4	10.43

The conductivity of investigated samples are approximately six times lower that of pure Cu (5.98×10^7 S/m at 20 °C [44]), so it can be concluded that the alloying of Cu with Al and Zn lowers the electrical conductivity.

This investigation focus was not on shape memory properties of these alloys, so it did not conduct experiments to determine the characteristic transformation temperatures of samples, but those of similar alloys from ternary Cu−Al−Zn system were previously investigated by KOSTOV and ŽIVKOVIĆ [45] using differential thermodilatometry.

5 Conclusions

1) The calculated Cu activities show negative deviation from the Rault's law at 1400 K, for both investigated section. The thermodynamic properties obtained by calculations indicate that Cu shows good miscibility with Al and Zn in all investigated alloys.

2) The microstructural analysis of investigated samples reveals that the structure consists of large and polygonal grains.

3) The EDX and XRD results reveal that the microstructure of investigated Cu-based shape memory alloys consist of solid solutions of Al in Cu and Zn in Cu, confirming the assumption based on knowledge about the phase diagram of constituent binary systems and the solid solubility of alloying metals in Cu.

4) It is found that increasing the Al content while reducing the Zn content leads to the decrease of hardness and electrical conductivity of the investigated alloys. The presented results contribute to better understanding of thermodynamic properties, microstructure, mechanical and electrical properties of Cu−Al−Zn-based shape memory alloys.

References

[1] MILOSAVLJEVIĆ A, KOSTOV A, TODOROVIĆ R. Smart materials: Shape memory alloys [J]. Bakar, 2011, 36(1): 39−44. (in Serbian)

[2] JANKE L, CZADERSKI C, MOTAVALLI M, RUTH J. Applications of shape memory alloys in civil engineering structures: Overview, limits and new ideas [J]. Materials and Structures, 2005, 38(5): 578−592.

[3] HUANG W M, DING Z, WANG C C, WEI J, ZHAO Y, PURNAWALI H. Shape memory materials [J]. Materials Today, 2010, 13(7−8): 54−61.

[4] CIMPOEŞU N, STANCIU S, VIZUREANU P, CIMPOEŞU R, CRISTIAN ACHIŢEI D, IONIŢĂ I. Obtaining shape memory alloy thin layer using PLD technique [J]. Journal of Mining and Metallurgy, Section B: Metallurgy, 2014, 50(1): 69−76.

[5] HUBER F, MELAND H, RØNNING M, VENVIK H, HOLMEN A. Comparison of Cu−Ce−Zr and Cu−Zn−Al mixed oxide catalysts for water-gas shift [J]. Topics in Catalysis, 2007, 45(1−4): 101−104.

[6] BREEN J P, ROSS J R H. Methanol reforming for fuel-cell applications: Development of zirconia-containing Cu−Zn−Al catalysts [J]. Catalysis Today, 1999, 51(3−4): 521−533.

[7] KANG N, SUNG NA H, JUN KIM S, YUN KANG C. Alloy design of Zn−Al−Cu solder for ultra-high temperatures [J]. Journal of Alloys and Compounds, 2009, 467(1−2): 246−250.

[8] MARTINEZ-FLORES E, NEGRETE J, TORRES VILLASENOR G. Structure and properties of Zn−Al−Cu alloy reinforced with alumina particles [J]. Materials and Design, 2003, 24(4): 281−286.

[9] CHEN Lu, YAN An, LIU Hua-shan, LI Xiao-qian. Strength and fatigue fracture behavior of Al−Zn−Mg−Cu−Zr(−Sn) alloys [J]. Transactions of Nonferrous Metals Society of China, 2013, 23(10): 2817−2825.

[10] LIU Jun-tao, ZHANG Yong-an, LI Xi-wu, LI Zhi-hui, XIONG Bai-qing, ZHANG Ji-shan. Thermodynamic calculation of high zinc-containing Al−Zn−Mg−Cu alloy [J]. Transactions of Nonferrous Metals Society of China, 2014, 24(5): 1481−1487.

[11] STIPCICH M, ROMERO R. The effect of post-quench aging on stabilization of martensite in Cu−Zn−Al and Cu−Zn−Al−Ti−B shape memory alloys [J]. Materials Science and Engineering A, 1999, 273−275: 581−585.

[12] ZHANG X M, LIU U M, FERNANDEZ J, GUILEMANY J M. Effect of small *g*-precipitates on the two-way shape memory effect in Cu−Zn−Al alloys [J]. Materials and Design, 2000, 21(6): 557−559.

[13] XU H, TAN S. Calorimetric investigation of a Cu−Zn−Al alloy with two way shape memory [J]. Scripta Metallurgica et Materialia, 2005, 33(5): 749−754.

[14] PELEGRINA J L, ROMERO R. Calorimetry in Cu−Zn−Al alloys under different structural and microstructural conditions [J]. Materials Science and Engineering A, 2000, 282(1−2): 16−22.

[15] CUNIBERTI A, ROMERO R. Differential scanning calorimetry study of deformed Cu−Zn−Al martensite [J]. Scripta Materialia, 2004, 51(4): 315−320.

[16] LONGAUER S, MAKROCZY P, JANAK G, LONGAUEROVA M. Shape memory effect in a Cu−Zn−Al alloy with dual phase α/β microstructure [J]. Materials Science and Engineering A, 1999, 273−275: 415−419.

[17] CEDERSTROM J, KOLOMYTSEV V, KOZLOV A, TITOV P, ZATULSKII G, KONDRATJUK S. Evolution of the shape memory parameters during multiple transformation cycles under load in Cu−Zn−Al alloys [J]. Materials Science and Engineering A, 1999,

273−275: 804−808.
[18] PONS J, MASSE M, PORTIER R. Thermomechanical cycling and two-way memory effect induced in Cu−Zn−Al [J]. Materials Science and Engineering A, 1999, 273−275: 610−615.
[19] AHMED M M. Corrosion behaviour of Zn−Al−Cu alloy in HCl solution and its inhibition [J]. Portugaliae Electrochimica Acta, 2006, 24: 1−22.
[20] LOJEN G, ANŽEL I, KNEISSL A, KRIŽMAN A, UNTERWEGER E, KOSEC B, BIZJAK M. Microstructure of rapidly solidified Cu−Al−Ni shape memory alloy ribbons [J]. Journal of Materials Processing Technology, 2012, 162−163: 220−229.
[21] SAVASKAN T, TURHAL M S. Relationships between cooling rate, copper content and mechanical properties of monotectoid based Zn−Al−Cu alloys [J]. Materials Characterization, 2003, 51(4): 259−270.
[22] CASOLCO S R, DOMINGUEZ G, SANDOVAL D, GARAY J E. Processing and mechanical behavior of Zn−Al−Cu porous alloys [J]. Materials Science and Engineering A, 2007, 471(1−2): 28−33.
[23] GOMIDZELOVIC L, POZEGA E, KOSTOV A, VUKOVIC N. Investigation of the structural, mechanical and electrical properties of Cu−Al−Zn shape memory alloys [J]. Materials Testing, 2014, 56(6): 486−489.
[24] LIANG H, CHANG Y A. A Thermodynamic description for the Al−Cu−Zn system [J]. Journal of Phase Equilibria, 1998, 19(1): 25−37.
[25] SEBKOVA J, KUBICEK L. Thermodynamic properties of a liquid zinc−aluminum−copper alloy [J]. Kovové Materialy, 1985, 23(1): 3−7.
[26] SUGINO S, HAGIWARA H. Activity of zinc in molten copper and copper−gold alloys [J]. Journal of the Japan Institute of Metals, 1986, 50(2): 1068−1074.
[27] VAN T D, SEGERS L, WINAND R. Determination of thermodynamic properties of ternary Al−Cu−Zn alloys by electromotive force method [J]. Journal of Electrochemical Society, 1994, 14(4): 927−933.
[28] MIETTINEN J. Thermodynamic description of the Cu−Al−Zn and Cu−Sn−Zn systems in the copper-rich corner [J]. Calphad, 2002, 26(1): 119−139.
[29] GOMIDŽELOVIĆ L, MIHAJLOVIĆ I, KOSTOV A, ŽIVKOVIĆ D. Cu−Al−Zn system: Calculation of thermodynamic properties in liquid phase [J]. Hemijska Industrija, 2013, 67(1): 157−164.
[30] GOMIDŽELOVIĆ L, KOSTOV A, ŽIVKOVIĆ D, POŽEGA E, KRSTIĆ V. Cu−Al−Zn system: Thermodynamic analisys by RKM model [J]. Bakar, 2013, 38(1): 1−10. (in Serbian)
[31] SEIFERT H J, LIANG P, LUKAS H L, ALDINGER F, FRIES S G, HAMERLIN M G, FAUDOT F, JANTZEN T. Computational phase studies in commercial aluminium and magnesium alloys [J]. Materials Science and Technology, 2000, 16(11−12): 1429−1433.
[32] ALDIRMAZ E, CELIK H, AKSOY I. SEM and X-ray diffraction studies on microstructures in Cu−26.04%Zn−4.01%Al alloy [J]. Acta Physica Polonica A, 2013, 124(1): 87−89.
[33] TOOP G W. Predicting ternary activities using binary data [J]. Transactions of the Society of Mining Engineers of AIME, 1965, 233(5): 850−854.
[34] MUGGIANU Y M, GAMBINO M, BROSS J P. Enthalpies of formation of liquid alloys [J]. Journal de Chimie Physique, 1975, 72(1): 83−88.
[35] WITUSIEWICZ V T, HECHT U, FRIES S G, REX S. The Ag–Al–Cu system: Part I: Reassessment of the constituent binaries on the basis of new experimental data [J]. Journal of Alloys and Compounds, 2004, 385(1−2): 133−143.
[36] DINSDALE G W, KROUPA A, VIZDAL J, VRESTAL J, WATSON A, ZEMANOVA A. COST 531 database for lead-free solders [DB]. Ver. 2.0, 2006.
[37] AN MEY S. Re-evaluation of the Al−Zn system [J]. Zeitschrift für Metallkunde, 1993, 84(7): 451−455. (in German)
[38] http://www.chemicalelements.com/elements/cu.html.
[39] ANDERSSON J O, HELANDER T, HÖGLUND L, SHI P F, SUNDMAN B. Thermo-Calc and DICTRA, computational tools for materials science [J]. Calphad, 2002, 26(2): 273−312.
[40] http://www.thermocalc.com.
[41] LUKAS H L, FRIES S G, SUNDMAN B. Computational thermodynamics: The Calphad method [M]. New York: Cambridge University Press, 2007.
[42] www.calphad.org.
[43] http://www. crct. polymtl. ca / fact / documentation / SGTE / SGTE_ Figs. htm.
[44] metals.about.com/od/properties/a/Electrical-Conductivity-In-Metals. htm.
[45] KOSTOV A, ŽIVKOVIĆ Ž. Thermo-dilatometry investigation of the martensitic transformation in copper-based shape memory alloys [J]. Thermochimica Acta, 1997, 291(1−2): 51−57.

Cu−Al−Zn 形状记忆合金的热力学性能和表征

Lidija GOMIDŽELOVIĆ[1], Emina POŽEGA[1], Ana KOSTOV[1], Nikola VUKOVIĆ[2], Vesna KRSTIĆ[1], Dragana ŽIVKOVIĆ[3], Ljubiša BALANOVIĆ[3]

1. Mining and Metallurgy Institute, Zeleni bulevar 35, Bor 19210, Serbia;
2. Faculty of Mining and Geology, University of Belgrade, Đušina 7, Belgrade 11000, Serbia;
3. Technical Faculty in Bor, University of Belgrade, VJ 12, Bor 19210, Serbia

摘　要：使用 Muggianu 模型计算 Cu−Al−Zn 三元形状记忆合金的热力学性能，通过实验研究其显微组织、硬度和导电性。使用 Thermo-Calc 软件计算 293 K 等温截面图，采用 X 射线衍射、光学显微镜、扫描电镜(SEM)和 X 射线能谱分析(EDX)、硬度和导电性测试对其性能进行表征。热力学计算结果表明：在所有研究合金中，Cu 与 Al 和 Zn 具有优良的混溶性。样品的显微结构分析表明其结构由大的多边形晶粒组成。

关键词：热力学；形状记忆合金；Cu−Al−Zn 合金；硬度；导电性　　**(Edited by Mu-lan QIN)**